Journal of Molecular Graphics and Modelling 28 (2009) 177–182

Contents lists available at ScienceDirect

Journal of Molecular Graphics and Modelling

journal homepage: www.elsevier.com/locate/JMGM

Solvolysis of chemical warfare agent VX is more efficient with hydroxylamine anion: A computational study

Md Abdul Shafeeuulla Khan [a], Manoj K. Kesharwani [a], Tusar Bandyopadhyay [b], Bishwajit Ganguly [a,*]

[a] Analytical Science Discipline, Central Salt & Marine Chemicals, Research Institute (Council of Scientific and Industrial Research), G.B. Marg, Bhavnagar 364002, Gujarat, India
[b] Theoretical Chemistry Section, Chemistry Group, Bhabha Atomic Research Centre Trombay, Mumbai 400085, India

ARTICLE INFO

Article history:
Received 8 April 2009
Received in revised form 16 June 2009
Accepted 19 June 2009
Available online 27 June 2009

Keywords:
Nerve agent
VX
Ab initio calculations
α-Nucleophiles
Hydroxylamine anion

ABSTRACT

The reaction of the chemical warfare agent VX with hydroxylamine anion (NH_2O^-) has been studied using a combination of correlated molecular orbital and density functional theory. It has been found that the hydroxylamine anion leads to predominant formation of non-toxic products for solvolysis of VX. The calculated activation barrier for the rate determining step of hydroxylamine anion with VX was found to be lower than that of hydroperoxidolysis and suggesting a more facile solvolysis with the former α-nucleophile. The conformational search was performed for VX using Monte Carlo search method with Merck Molecular force fields (MMFFs), which lead to a more stable conformation than reported. The anomeric effect operates in the lowest energy conformation of VX and contributes towards its stabilization. The reactivity of the α-nucleophiles towards VX was correlated well with the corresponding charges on nucleophilic oxygen atoms.

1. Introduction

VX (*O*-ethyl *S*-[2-(diisopropylamino)ethyl] methylphosphonothiolate) is one of the extremely toxic nerve agents belonging to V-series. Due to its non-volatile nature, VX is highly persistent compared to G-series nerve agents [1,2]. Binding of VX to the acetyl cholinesterase enzyme (AChE) leads to cause asphyxiation [3]. VX can enter the system not only by inhalation but also through penetrating the skin [3]. Thus efficient methods for detoxification of VX are needed. Detoxification of nerve agents is an important area of research since decades. Many experimental as well as theoretical studies have been performed to explore the pathways for the destruction mechanism of VX [4–11]. Two possible ways to destroy the VX is breaking of phosphorus–sulfur bond (P–SR, where R is 2-(diisopropylamino) ethyl) or cleavage of phosphorus–ethoxide (P–OEt) bond [4]. Breaking of P–OEt bond is still harmful as it results in the production of another neurotoxin thiocolic acid derivative EA2192 (*S*-(2-diisopropylamino) ethyl methylphosphonothioic acid) [4,12]. Thus nucleophiles which predominantly cleave P–SR bond of VX will be more useful as a detoxifying reagent.

The simple alkaline hydrolysis of VX is slow and results in a mixture of neurotoxic and non-toxic products [1,10]. Use of α-nucleophiles has shown to be effective for the destruction of organophosphorus nerve agents [7]. A theoretical study on solvolysis of VX using hydroxide and α-nucleophile hydroperoxide was reported [9]. It was found that hydroperoxide is a better nucleophile compared to hydroxide as hydroperoxidolysis solely leads to the formation of non-toxic products [9]. Recently, (–N–O^- type) α-nucleophiles, i.e., hydroxybenzotriozoles have also been used for the solvolysis of toxic organophosphate esters [13]. The rate of solvolysis of such toxic esters is faster with these (–N–O^- type) α-nucleophiles and the observed results are explained based on the nucleophilic charges in the study [13]. These results prompted us to explore the solvolysis of VX with (–N–O^- type) α-nucleophiles, which can also be a better nucleophile. In the present work, we have reported the destruction mechanism of VX with hydroxylamine anion (NH_2O^-) as a (–N–O^-) α-nucleophile. The charge analysis of nucleophilic oxygens of NH_2O^- and HO_2^- suggest that the oxygen atom of NH_2O^- carries more negative charge than that of hydroperoxy oxygen (Scheme 1). Therefore, based on the charge analysis, NH_2O^- can act as a more potent nucleophile compared to HO_2^- for the destruction of VX. However, it is important to quantitatively estimate the activation barriers on the potential energy surface for NH_2O^- and VX for a direct comparison with the HO_2^- α-nucleophile. The detailed solvolysis pathways for the destruction of VX with NH_2O^- are discussed in this study.

2. Computational methods

Monte Carlo conformational Search (MC) [14] was performed for VX using (MMFFs) [15] Force Field in gas phase for 5000 steps

* Corresponding author. Tel.: +91 278 2567760x677; fax: +91 278 2567562.
E-mail address: ganguly@csmcri.org (B. Ganguly).

1093-3263/$ – see front matter © 2009 Elsevier Inc. All rights reserved.
doi:10.1016/j.jmgm.2009.06.004

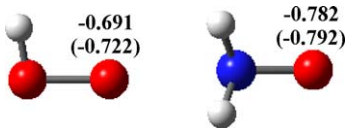

Scheme 1. MPW1K/MIDI! calculated mulliken and natural charges (·) for the anionic oxygens in hydroperoxide and hydroxylamine anions (red = oxygen; blue = nitrogen; white = hydrogen).

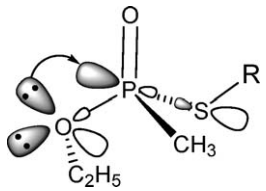

Scheme 2. Stereoelectronic interaction between n(O1) lone pair and σ*(P–S) orbital.

yielded 104 unique conformations, however, 47 conformers were minimized with good convergence. We selected only 7 unique conformers out of 47 minimized geometries based on structural and energetic criteria for higher level DFT [16] calculations. Similarly, the MC search performed in the aqueous phase using Generalized-Born/Surface-Area (GB/SA) [17] model leads to 223 unique conformations, whereas, 93 structures minimized with good convergence. Out of 93 minimized geometries, we selected 7 unique structures for higher level (DFT) calculations. All 14 force field conformations were fully optimized with MPW1K [18] density functional and the MIDI! [19] basis set in gas phase. Harmonic frequency calculations were carried out at the same level of theory to confirm the stationary points and for thermodynamic corrections. Intrinsic reaction coordinate (IRC) [20] calculations were performed to examine that the transition states connect to their respective minima. Single point calculations at the MP2/6−31+G(d) [21,22] level of theory using MPW1K optimized geometries. Free energies of solvation in aqueous phase were calculated with the gas-phase optimized structures at the HF/6−31+G(d) level of theory with integral equation formalism polarizable continuum model (IEF-PCM) [23] using the UFF radii [24]. All energies discussed are solvated enthalpies corrected to 298 K. All calculations were performed using Gaussian 03, Revision E.01 program [25].

3. Results and discussion

To consider the reaction mechanism of VX with NH_2O^-, we have performed the conformational search for the lowest energy conformer of VX using MMFFs method and density functional calculations with MPW1K/MIDI! method. The lowest energy conformer predicted for VX using MMFFs and MPW1K/MIDI! methods was found to be energetically more stable by 1.4 kcal/mol than that of the reported conformer employed for the study with hydroxide and hydroperoxide ions [9]. The major difference lies in the torsion angles (C1–S2–P3–O4) between the lowest energy conformer (**a**) and the reported one (**b**). In the case of **a** the calculated torsion angle is 72.0°, whereas, the corresponding angle for **b** is 163.0° (Fig. 1). Consequently, the anomeric [26–32] type interaction is possible between the n(O1) lone-pair and the σ*(P–S) orbital in the newly searched conformation **a** (Scheme 2). Such a possibility does not arise for **b**. The second order perturbation calculations with NBO method [33] shows that the n(O1) lone-pair and the σ*(P–S) orbital interaction energy is (1.70 kcal/mol) higher for **a** than that of **b**. Therefore, it appears that the anomeric effect seems to be one of the major factors towards the stabilization of newly searched VX than the reported structure. In the present study, we have used the lowest energy conformation of VX for the solvolysis with NH_2O^- anion.

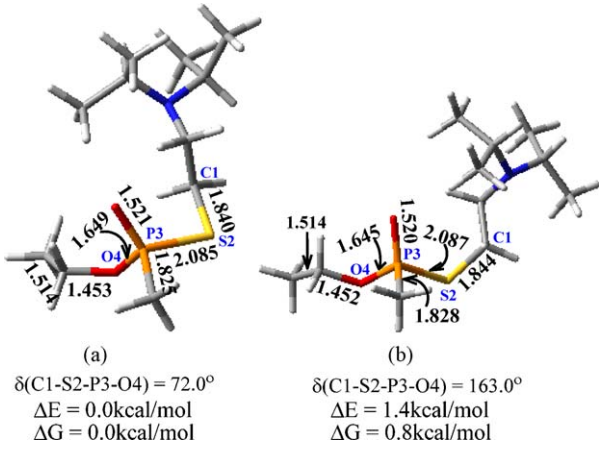

Fig. 1. (**a**) Lowest energy conformation of VX obtained from Monte Carlo conformational search using MMFFs force field and DFT (MPW1K/MIDIx). (**b**) VX conformation reported with MPW1K/MIDIx (Ref. [9]).

The solvolysis of organophosphorus nerve agents is believed to proceed through the formation of a trigonal bipyramidal (TBP) intermediates [34]. In general, the most electronegative group thermodynamically prefer the apical position in trigonal bipyramidal phosphorus compounds, and also elimination is more facile from an apical position [35]. Thus, the most electronegative group may be expected to be the preferred leaving group in the absence of any other electronic or steric reasons. In the case of VX, ethoxide ion is more electronegative compared to that of thiolate group and therefore more apicophilic; however, thiolates are less basic than ethoxide ion therefore, can be a good leaving group [36]. This leads to a competition between the cleavages of a P–O and P–S bonds depending upon the nature of nucleophile and reaction conditions. We have considered both the pathways for solvolysis of VX. First one is attack of nucleophile opposite to thiolate ligand (Path A) and other one is opposite to ethoxide group (Path B). The energy profile diagrams for these pathways are given in Fig. 2.

Hydroxylamine anion (NH_2O^-) attack opposite to thiolate group of VX leads to formation of transition state **TS1a**, with an activation barrier of 7.4 kcal/mol. It should be noted that activation barrier calculated with hydroperoxide and VX was 10.2 kcal/mol at the same level of theory [9], which is higher than the barrier calculated with NH_2O^- anion. Since this is the rate determining step for the P–S bond cleavage, the NH_2O^- anion seems to be a more potent α-nucleophile compared to that of hydroperoxide. Transition state **TS1a** further proceeds to trigonal bipyramidal intermediate geometry **1a** which is 8.2 kcal/mol below the reactant molecules (Fig. 2). Further, the cleavage of P–S bond proceeds through another transition state **TS2a** with an activation barrier of −4.0 kcal/mol (Fig. 2). IRC calculations confirm that **TS2a** connects to **1a**. Thus, the discrepancy that **TS2a** lies below **1a** is likely due to the fact that gas phase energies were refined with the free energy of solvation. The true solvated stationary points showed the positive barrier for **TS2a** on the reaction coordinate (Fig. S1 in Supplementary data). Earlier studies on the nucleophilic substitution at different reaction centers (C, Si and P) have shown that solvation drastically changes the reaction profiles in particular a positive activation energies to the products [37–39]. Finally, the cleavage of P–SR bonds results in exothermic non-toxic products **Pa** (ethyl aminooxy(methyl)-phosphinate) and **RS**$^-$ (2-(diisopropylamino) ethanethiolate), which are collectively 30.3 kcal/mol lower in energy than the reactants (Fig. 2).

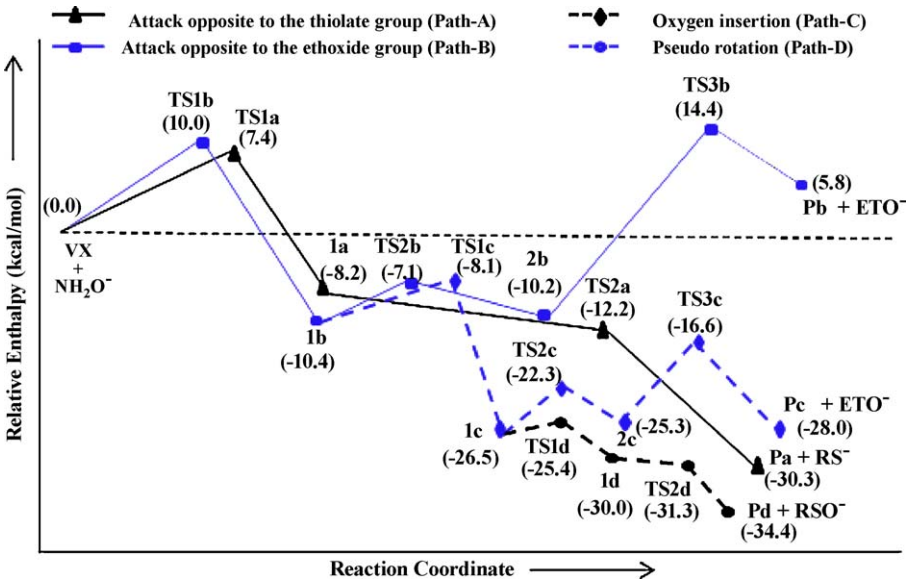

Fig. 2. Energy profile diagram for reaction between VX and hydroxylamine anion nucleophile.

The calculated transition state and intermediate structures of P–S bond cleavage for VX with NH_2O^- anion are shown in Fig. 3. In the transition state **TS1a**, the P–ONH_2 and P–SR bond lengths are of 2.813 and 2.144 Å, respectively. In TBP intermediate **1a** the corresponding P–ONH_2 bond become closure and P–SR bond lengthens compared to the transition state **TS1a** (Fig. 3). In the second transition state **TS2a**, the P–ONH_2 bond further shortens to 1.683 Å and P–SR bond lengthens to 3.151 Å (Fig. 3) showing bonding of oxygen with phosphorus and leaving of –SR group.

In the Path B, attack of the NH_2O^- anion opposite to the ethoxide ligand forms the transition state **TS1b** with P–ONH_2 and P–OEt bond distances 2.846 and 1.680 Å, respectively (Fig. 3). The activation enthalpy calculated with respect to the reactants for **TS1b** is 10.0 kcal/mol, which is 2.6 kcal/mol higher compared to

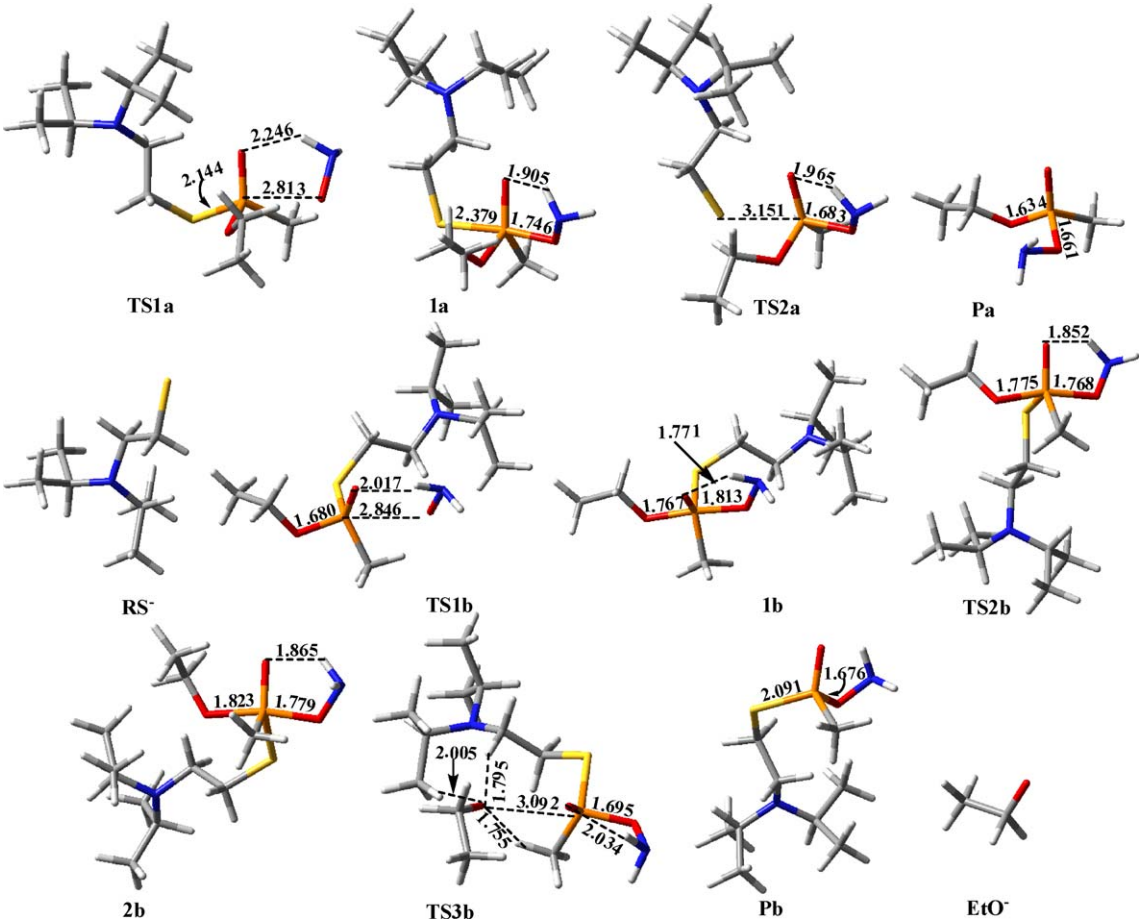

Fig. 3. MPW1K/MIDI! optimized stationary points involved in the solvolysis of VX with hydroxylamine anion (Paths A and B).

the thiolate activation enthalpy **TS1a** (Fig. 3). To note that the activation enthalpy with hydroperoxide and VX is 12.9 kcal/mol, which is again higher than the activation enthalpy of NH_2O^- anion with VX for the attack opposite to ethoxide group [9]. The resultant intermediate **1b** lying 10.4 kcal/mol below the reactants. Intermediate **1b** undergoes a conformational reorganization into another intermediate **2b** through the transition state **TS2b** with a small activation enthalpy (3.3 kcal/mol) via rotation along the P–S bond. The entire process arranges the diisopropylamino group such that it can stabilize the leaving group via (C–H···O) type hydrogen bonding with oxygen of the leaving group. Further, leaving of ethoxide group proceeds via the transition state **TS3b** with much higher activation enthalpy (24.6 kcal/mol). In transition state geometry **TS3b**, the P–OEt and P–ONH_2 distances are 3.092 and 1.695 Å, respectively. The overall removal process of ethoxide group leads to the formation of toxic product **Pb** (*S*-2-(diisopropylamino)ethylaminooxy(methyl) phosphinothioate), which is endothermic by 5.8 kcal/mol. The higher activation enthalpy for the transition state **TS3b** and endothermicity of whole process makes the Path B reversible. To note that the comparison shown here between hydroperoxydolysis [9] and solvolysis with hydroxylamine anion was made with two different VX conformers. To examine the change in relative energies for hydroperoxidolysis with the lowest energy conformer of VX ascertained in this study, we have located the corresponding stationary points **TS1a**, **TS1b** and **TS3b** for the attack of hydroperoxide. The calculated activation barriers for these corresponding points were found to be 7.9, 7.6 and 27.1 kcal/mol, respectively. The barriers estimated for **TS1a**, and **TS1b** with the new conformation of VX seems to much lower than the one calculated earlier [9] (Fig. S2 in Supplementary data).

These calculations borne out some interesting trends to compare the pathways A and B, respectively for hydroperoxidolysis of VX and solvolysis with hydroxylamine anion. Following a Curtin–Hammett analysis, the 0.3 kcal/mol difference in activation enthalpies between **TS1a** and **TS1b** for hydroperoxidolysis indicates 2:1 preference for initial peroxide attack opposite to the ethoxide ligand, which leads to toxic products [40]. The inherent error involved in this level of theory is approximately ±1 kcal/mol, it is reasonable to conclude that the Paths A and B would be competitive in this case. The activation enthalpy difference for **TS1a** and **TS1b** for solvolysis with hydroxylamine anion is 2.6 kcal/mol indicates 78:1 preference for initial NH_2O^- attack opposite to the thiolate ligand leads to non-toxic product. The corresponding rate constants k (s^{-1}) calculated using Arrhenius equation for the non-toxic products obtained with hydroperoxidolysis and NH_2O^- are 1.75×10^{-6} and 4.05×10^{-6}, respectively.

Another possibility from trigonal bipyramidal intermediate **1b** was found to undergo an internal oxygen insertion preferentially as in the case of hydroperoxidolysis (Path C) [9]. The nucleophilic oxygen of the NH_2O^- anion inserts between the P and S atoms through a three membered ring transition state **TS1c**. In **TS1c**, the N–O, O–S and P–N bond distances are 1.842, 2.308 and 2.262 Å, respectively. These geometrical parameters in the **TS1c** show that the oxygen of the NH_2O^- anion is in the process of insertion in between the phosphorus and sulfur atoms and the amino group of anion migrates to the phosphorus atom. The transition state **TS1c** leads to the formation of intermediate **1c**, which is 26.5 kcal/mol below reactants. In **1c**, the P–NH_2, P–OS and O–S bond distances are 1.838, 1.740 and 1.684 Å, respectively suggesting the insertion of oxygen between phosphorus and sulfur atoms (Fig. 4). The

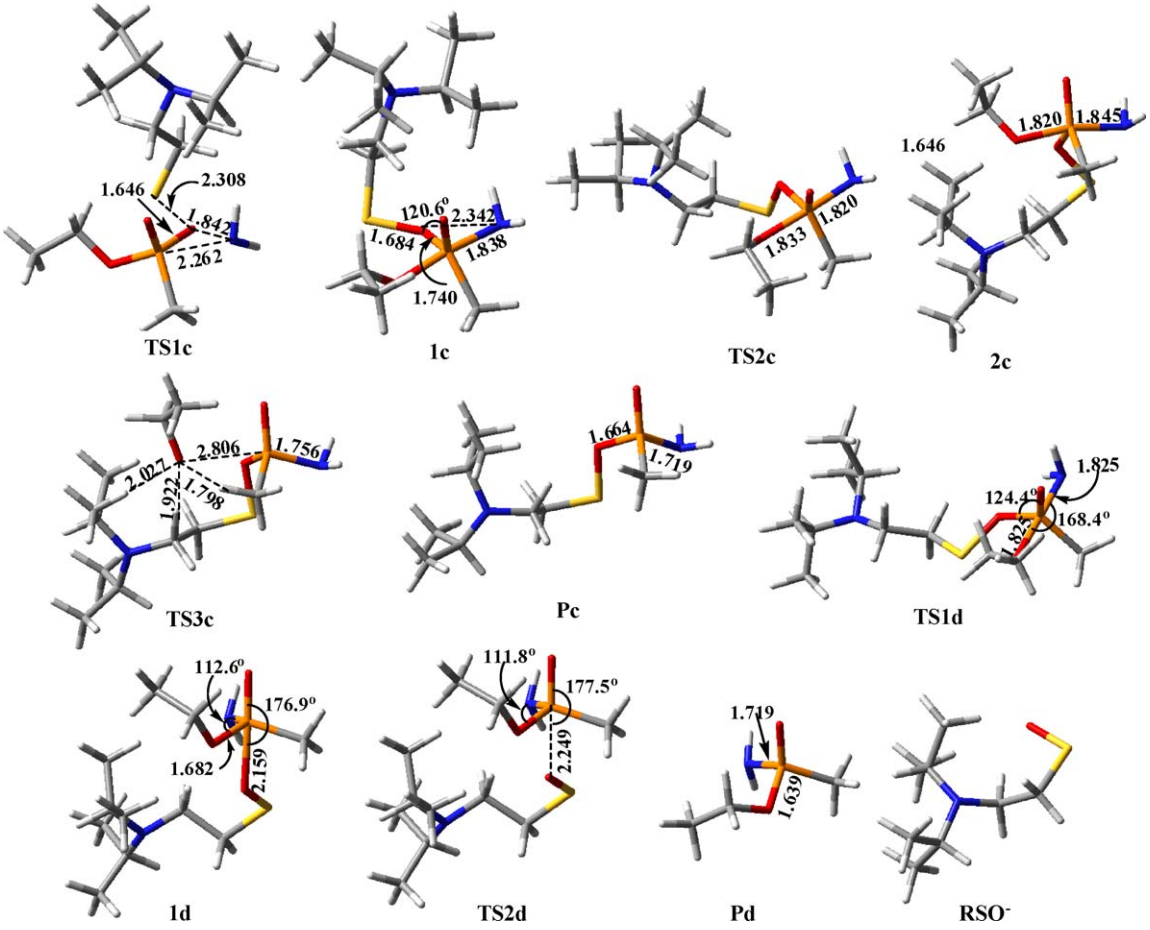

Fig. 4. MPW1K/MIDI! optimized stationary points involved in the solvolysis of VX with hydroxylamine anion (Paths C and D).

intermediate **1c** can move to **2c** via a rotational transition state **TS2c**. The calculated activation enthalpy is 4.2 kcal/mol (Fig. 2). From **1c** to **2c**, there is no significant change in the P–OEt and P–NH_2 bond distances. Further, the expulsion of ethoxide group proceeds through the transition state **TS3c** to form products **Pc** (*OS*-2-(diisopropylamino)ethyl *P*-methylphosphonamido(thioperoxoate)) and ethoxide ion (**EtO**$^-$). The stabilization of the leaving group in **TS3c** comes through a C–H···O type interaction between diisopropylamine group and the oxygen of the leaving ethoxide group. It is not clear whether product **Pc** would retain neurotoxicity (Fig. 4).

Trigonal bipyramidal intermediate **1c** can undergo pseudorotation (Path D), which can place the (P–O$^-$) oxygen and oxysulfenate ligand in apical position **1d**. The pseudorotational transition state **TS1d** lies at −25.4 kcal/mol below reactants, while TBP intermediate **1d** is −30.0 kcal/mol lower compared to reactants (Fig. 2). The expulsion of oxysulfenate group is barrierless to form the products. The overall energetics is exergonic for this pseudorotational process and leads to non-toxic products. While we were working on the solvolysis of VX with NH_2O^- anion, we came across a paper appeared very recently corroborating our claim of facile detoxification of organophosphorus esters [41].

4. Conclusions

Computational study has been carried out on the solvolysis of VX with hydroxylamine anion at the MP2/6−31+G(d)//MPW1K/MIDI! + IEF−PCM(HF/6−31+G(d)) level of theory. The conformation search protocol employed in this study yielded a lower energy conformer than the reported one. The newly searched conformer seems to stabilize through stereoelectronic effect. Using the lowest energy conformer of VX searched in this study, we have found that the formation of non-toxic products with hydroxylamine anion (NH_2O^-) is kinetically favored than that of the reported hydroperoxidolysis at the same level of theory. The pathway which leads to toxic products was found to be unfavorable both kinetically and thermodynamically with hydroxylamine anion. Oxygen insertion leads to two competitive pathways in which P–OSR cleavage leads to completely non-toxic products and the P–OEt cleavage leads to products of which the toxicity is still not clear. The activation barrier of the P–OSR cleavage in the case of hydroxylamine nucleophile was found to be lower than that of the P–OSR cleavage for hydroperoxide. The calculated results show that hydroxylamine anion should act as a more potent nucleophile for the solvolysis of VX compared to hydroperoxide. The nucleophilic charges calculated for the α-nucleophiles correlate well with their reactivity towards the solvolysis of VX as a case study.

Acknowledgments

Authors thank DAE-BRNS, Mumbai, India, for financial support of this work. Author MASK is thankful to DAE-BRNS and MKK is thankful to UGC, New Delhi, India, for awarding fellowship. We thank the reviewers for their comments and suggestions that have helped us to improve the paper.

Appendix A. Supplementary data

Supplementary data associated with this article can be found, in the online version, at doi:10.1016/j.jmgm.2009.06.004.

References

[1] Y.-C. Yang, J.A. Baker, J.R. Ward, Decontamination of chemical warfare agents, Chem. Rev. 92 (1992) 1729–1743.
[2] M. Somani, Chemical Warfare Agents, Academic Press, San Diego, CA, 1992.
[3] H.P. Benschop, L.P.A. De Jong, Nerve agent stereoisomers: analysis, isolation and toxicology, Acc. Chem. Res. 21 (1988) 368–374.
[4] Y.-C. Yang, Chemical detoxification of nerve agent VX, Acc. Chem. Res. 32 (1999) 109–115 (and references therein).
[5] Y.C. Yang, L.L. Szafraniec, W.T. Beaudry, D.K. Rohrbaugh, L.R. Procell, J.B. Samuel, Autocatalytic hydrolysis of V-type nerve agents, J. Org. Chem. 61 (1996) 8407–8413.
[6] J.M. Williams, B. Rowland, M.T. Jeffery, G.S. Groenewold, A.D. Appelhans, G.L. Gresham, J.E. Olson, Degradation kinetics of VX on concrete by secondary ion mass spectrometry, Langmuir 21 (2005) 2386–2390.
[7] T. Cassagne, H.-J. Cristau, G. Delmas, M. Desgranges, C. Lion, G. Magnaud, É. Torreilles, D. Virieux, Destruction of chemical warfare agents VX and soman by α-nucleophiles as oxidizing agents, Heteroat. Chem. 12 (2001) 485–490.
[8] J. Šečkutė, J.L. Menke, R.J. Emnett, E.V. Patterson, C.J. Cramer, Ab initio molecular and density functional studies on the solvolysis of sarin and O,S-dimethyl methylphosphonothiolate, a VX-like compound, J. Org. Chem. 70 (2005) 8649–8660.
[9] K.A. Daniel, L.A. Kopff, E.V. Patterson, Computational studies on the solvolysis of the chemical warfare agent VX, J. Phys. Org. Chem. 21 (2008) 321–328.
[10] J. Epstein, J.J. Callahan, V.E. Bauer, The kinetics and mechanisms of hydrolysis of phosphonothiolates in dilute aqueous solution, Phosphorus 4 (1974) 157–163.
[11] E. Gershonov, I. Columbus, Y. Zafrani, Facile hydrolysis-based chemical destruction of the warfare agents VX, GB, and HD by alumina-supported fluoride reagents, J. Org. Chem. 74 (2009) 329–338.
[12] Y.-C. Yang, L.L. Szafraniec, W.T. Beaudry, D.K. Rohrbaugh, Oxidative detoxification of phosphonothiolates, J. Am. Chem. Soc. 112 (1990) 6621–6627.
[13] P.V. Kumar, B. Ganguly, S. Bhattacharya, Computational study on hydroxybenzotriazoles as reagents for ester hydrolysis, J. Org. Chem. 69 (2004) 8634–8642.
[14] G. Chang, W.C. Guida, W.C. Still, An internal-coordinate Monte Carlo method for searching conformational space, J. Am. Chem. Soc. 111 (1989) 4379–4386.
[15] T.A. Halgren, Merck molecular force field. I. Basis, form, scope, parameterization, and performance of MMFF94, J. Comput. Chem. 17 (1996) 490–519.
[16] P. Hohenberg, W. Kohn, Inhomogeneous electron gas, Phys. Rev. 136 (1964) B864–B871.
[17] W.C. Still, A. Tempczyk, R.C. Hawlely, T. Hendrickson, Semianalytical treatment of solvation for molecular mechanics and dynamics, J. Am. Chem. Soc. 112 (1990) 6127–6129.
[18] B.J. Lynch, D.G. Truhlar, How well can hybrid density functional methods predict transition state geometries and barrier heights? J. Phys. Chem. A 105 (2001) 2936–2941.
[19] R.E. Easton, D.J. Giesen, A. Welch, C.J. Cramer, D.G. Truhlar, The MIDI! basis set for quantum mechanical calculation of molecular geometries and partial charges, Theor. Chem. Acc. 93 (1996) 281–301.
[20] C. Gonzalez, H.B. Schlegel, An improved algorithm for reaction path following J, Chem. Phys. 90 (1989) 2154–2161.
[21] C. Møller, M.S. Plesset, Note on an approximation treatment for many-electron systems, Phys. Rev. 46 (1934) 618–622.
[22] W.J. Hehre, L. Radom, P.v.R. Schleyer, J.A. Pople, Ab Initio Molecular Orbital Theory, Wiley Interscience, New York, 1986.
[23] M.T. Cancès, B. Mennucci, J. Tomasi, A new integral equation formalism for the polarizable continuum model: theoretical background and applications to isotropic and anisotropic dielectrics, J. Chem. Phys. 107 (1997) 3032–3041.
[24] A.K. Rappé, C.J. Casewit, K.S. Colwell, W.A. Goddard III, W.M. Skiff, UFF, a full periodic table force field for molecular mechanics and molecular dynamics simulations, J. Am. Chem. Soc. 114 (1992) 10024–10035.
[25] M.J. Frisch, G.W. Trucks, H.B. Schlegel, G.E. Scuseria, M.A. Robb, J.R.J. Cheeseman, A. Montgomery Jr., T. Vreven, K.N. Kudin, J.C. Burant, J.M. Millam, S.S. Iyengar, J. Tomasi, V. Barone, B. Mennucci, M. Cossi, G. Scalmani, N. Rega, G.A. Petersson, H. Nakatsuji, M. Hada, M. Ehara, K. Toyota, R. Fukuda, J. Hasegawa, M. Ishida, T. Nakajima, Y. Honda, O. Kitao, H. Nakai, M. Klene, X. Li, J.E. Knox, H.P. Hratchian, J.B. Cross, V. Bakken, C. Adamo, J. Jaramillo, R. Gomperts, R.E. Stratmann, O. Yazyev, A.J. Austin, R. Cammi, C. Pomelli, J.W. Ochterski, P.Y. Ayala, K. Morokuma, G.A. Voth, P. Salvador, J.J. Dannenberg, V.G. Zakrzewski, S. Dapprich, A.D. Daniels, M.C. Strain, O. Farkas, D.K. Malick, A.D. Rabuck, K. Raghavachari, J.B. Foresman, J.V. Ortiz, Q. Cui, A.G. Baboul, S. Clifford, J. Cioslowski, B.B. Stefanov, G. Liu, A. Liashenko, P. Piskorz, I. Komaromi, R.L. Martin, D.J. Fox, T. Keith, M.A. Al-Laham, C.Y. Peng, A. Nanayakkara, M. Challacombe, P.M.W. Gill, B. Johnson, W. Chen, M.W. Wong, C. Gonzalez, J.A. Pople, Gaussian 03, Revision E.01, Gaussian Inc., Wallingford, CT, 2004.
[26] A.J. Kirby, The Anomeric Effect and Related Stereoelectronic Effects at Oxygen, Springer Verlag, Berlin, 1983.
[27] Anomeric effect, origin and consequences, W.A. Szarek, D. Horton (Eds.), ACS Symposium Series No. 87, American Chemical Society, Washington, DC, 1979.
[28] P. Deslongchamps, Stereoelectronic Effect in Organic Chemistry, Wiley, New York, 1983.
[29] The Anomeric effect and Associated Stereoelectronic effects, G.R.J. Thatcher (Ed.), ACS Symposium Series No. 539, American Chemical Society, Washington, DC, 1993.
[30] R.U. Lemieux, in: P. de Mayo (Ed.), Molecular Rearrangements, vol. III, Interscience, New York, 1964, p. 709.
[31] B. Ganguly, B. Fuchs, Stereoelectronic effects in negatively and positively (protonated) charged species. Ab Initio studies of the anomeric effect in 1,3-dioxa systems, J. Org. Chem. 62 (1997) 8892–8901.
[32] E.A. Ruben, J.A. Plumley, M.S. Chapman, J.D. Evanseck, Anomeric effect in "high energy" phosphate bonds. Selective destabilization of the scissile bond and

modulation of the exothermicity of hydrolysis, J. Am. Chem. Soc. 130 (2008) 3349–3358.
[33] J.P. Foster, F. Weinhold, Natural hybrid orbitals, J. Am. Chem. Soc. 102 (1980) 7211–7218.
[34] F. Zheng, C.-G. Zhan, R.L. Ornstein, Theoretical studies of reaction pathways and energy barriers for alkaline hydrolysis of phosphotriesterase substrates paraoxon and related toxic phosphofluoridate nerve agents, J. Chem. Soc., Perkin Trans. 2 (2001) 2355–2363.
[35] G.R.J. Thatcher, R. Kluger, Adv. Phys. Org. Chem. 25 (1989) 99.
[36] R.G. Cavell, J.A. Gibson, K.I. The, Phosphoranes. 8. Dynamic ^{13}C NMR studies of a series of fluxional tetraalkylphosphoranes $(CF_3)_3CH_3PY$ [Y = F, Cl, OCH_3, SCH_3 $N(CH_3)_2$], Inorg. Chem. 17 (1978) 2880–2885.
[37] M.A. van Bochove, F.M. Bickelhaupt, Nucleophilic Substitution at C, Si and P: how solvation affects the shape of reaction profiles, Eur. J. Org. Chem. (2008) 649–654.
[38] M.A. van Bochove, M. Swart, F.M. Bickelhaupt, Nucleophilic substitution at phosphorus centers ($S_N2@P$), Chem. Phys. Chem. 8 (2007) 2452–2463.
[39] M.A. van Bochove, M. Swart, F.M. Bickelhaupt, Nucleophilic substitution at phosphorus ($S_N2@P$): disappearance and reappearance of reaction barriers, J. Am. Chem. Soc. 128 (2006) 10738–10744.
[40] F.A. Carey, R.J. Sundberg, Advanced Organic Chemistry. Part A. Structure and Mechanisms, 4th edition, 2000, pp. 220–222.
[41] A.J. Kirby, A.M. Manfredi, B.S. Souza, M. Medeiros, J.P. Priebe, T.A.S. Brandao, F. Nome, Reactions of alpha-nucleophiles with a model phosphate diester, ARKIVOC (2009) 28–38 (and references therein).